RAPID COMMUNICATIONS

PHYSICAL REVIEW B **85**, 140508(R) (2012)

Reentrant topological transitions in a quantum wire/superconductor system with quasiperiodic lattice modulation

Masaki Tezuka* and Norio Kawakami

Department of Physics, Kyoto University, Kitashirakawa, Sakyo-ku, Kyoto 606-8502, Japan

(Received 1 March 2012; published 16 April 2012)

We study the condition for a topological superconductor (TS) phase with end Majorana fermions to appear when a quasiperiodic lattice modulation is applied to a one-dimensional quantum wire with strong spin-orbit interaction situated under a magnetic field and in proximity to a superconductor. By density-matrix renormalization group analysis, we find that multiple topological phases with Majorana end modes are realized in finite ranges of the filling factor, showing a sequence of reentrant transitions as the chemical potential is tuned. The locations of these phases reflect the structure of bands in the noninteracting case, which exhibits a distinct self-similar structure. The stability of the TS in the presence of an on-site interaction or a harmonic trap potential is also discussed.

DOI: 10.1103/PhysRevB.85.140508 PACS number(s): 74.90.+n, 71.10.Pm, 03.65.Vf, 67.85.−d

Edge states of topologically nontrivial systems have attracted attention because they are *topologically protected*, that is, they are stable against weak perturbations that do not change the topology of their quantum state. Majorana surface states can form at the boundaries or vortex cores of topological superconductors (TSs),[1–6] and there has been a large amount of effort to observe such states partly because they are expected to be useful in realizing quantum computation.[2,7] The TS can form in a one-dimensional (1D) quantum wire with spin-orbit interaction (SOI) that is placed under a Zeeman field and close to a bulk superconductor,[8–11] or in cold atoms in two-dimensional optical lattices with effective gauge fields generated by spatially varying laser fields,[5] among others.

Here we are interested in the effect of spatial inhomogeneity of the system,[12,13] imposed as a modification of site energy levels, on the realization of Majorana end states. Recently, Brouwer and coworkers[14] have studied two models, the Dirac equation with random mass and a 1D spinless superconductor, and obtained the energy distributions of the end states. The end modes of noninteracting 1D systems with quasiperiodic potentials have also been studied in connection with two-dimensional integer quantum Hall systems[15] and quantum spin Hall systems.[16]

There is also a growing interest in the role of the electron-electron interaction in 1D conductors with SOI and topological materials.[17–22] Stoudenmire and coworkers[20] showed that while an on-site electron-electron interaction U reduces the proximity-induced superconducting gap on a quantum wire attached to a bulk superconductor, the chemical potential range of a TS with Majorana end states is enlarged by $U > 0$.

In this work, we study the effect of a quasiperiodic site level modification of a 1D lattice. Such a system has been realized in cold-atom systems[23,24] and can also be relevant when the quantum wire is placed on a bulk superconductor which has the lattice (or superlattice) constant incommensurate with that of the quantum wire. We find that TSs with Majorana end states are observed in several regions with finite widths of the chemical potential closer to the band center, which resembles the multichannel case.[22,25,26] Moreover, those TS regions are broadened by $U > 0$. This result paves a way to the observation and manipulation of Majorana end states in various 1D TS systems with inhomogeneities, which may be tunable or unavoidable.

Setup. We study a tight-binding 1D fermion model by the density-matrix renormalization group (DMRG).[27,28] Up to 160 eigenstates of the reduced density matrix ρ, with the sum of discarded eigenvalues of ρ at each step in the last finite-size system loop being typically less than 10^{-7}, have been retained in the DMRG calculation.

We adopt the following Hamiltonian:

$$\begin{aligned}\mathcal{H} = &-\frac{t}{2}\sum_{l=0}^{L-2}\sum_{\sigma=\uparrow,\downarrow}(\hat{c}^\dagger_{\sigma,l}\hat{c}_{\sigma,l+1} + \text{h.c.}) \\ &+ U\sum_{l=0}^{L-1}\hat{n}_{\uparrow,l}\hat{n}_{\downarrow,l} + \Delta\sum_{l=0}^{L-1}(\hat{c}_{\uparrow,l}\hat{c}_{\downarrow,l} + \text{h.c.}) \\ &+ \sum_{l=0}^{L-1}\Bigg[V_z(\hat{n}_{\uparrow,l} - \hat{n}_{\downarrow,l}) + \sum_{\sigma=\uparrow,\downarrow}(t - \mu + \epsilon_{\sigma,l})\hat{n}_{\sigma,l}\Bigg] \\ &+ \frac{\alpha}{2}\sum_{l=0}^{L-2}[(\hat{c}^\dagger_{\downarrow,l}\hat{c}_{\uparrow,l+1} - \hat{c}^\dagger_{\uparrow,l}\hat{c}_{\downarrow,l+1}) + \text{h.c.}]. \end{aligned} \tag{1}$$

Here, $\hat{c}_{\sigma,l}$ annihilates a fermion with spin $\sigma(=\uparrow, \downarrow)$ at site $l(=0,1,\ldots,L-1)$, $\hat{n}_{\sigma,l} \equiv \hat{c}^\dagger_{\sigma,l}c_{\sigma,l}$, t is the nearest-neighbor hopping, U is the on-site interaction, Δ is the coupling to the bulk superconductor, α is the Rashba-type SOI, V_z is the Zeeman energy, and μ is the chemical potential. In the following, we set $L = 200$ and $t = 1$. We take $(\Delta,\alpha,V_z) = (0.1,0.3,0.3)$ unless noted otherwise, as in Figs. 2, 3, and 6 of Ref. 20. $\epsilon_{\sigma,l} = \epsilon_l$ is the site energy for spin σ on site l.

For an infinite-size system with $U = \Delta = 0$ and $\epsilon_{\uparrow,l} = 0$, it is straightforward to obtain the single-particle dispersion relation as a function of the quasimomentum k:

$$E^{\pm}(k) = t[1 - \cos(k)] \pm \sqrt{\alpha^2\sin^2(k) + V_z^2}. \tag{2}$$

In this Rapid Communication, we call them the upper and lower Rashba–Zeeman (RZ) bands.

If the Hamiltonian can be mapped to that of a spinless system, the TS state is realized by the introduction of the pairing Δ. When $\Delta \ll V_z$, such mapping is possible if μ is in only one of the RZ bands.[10,11,20] For a more general discussion on the origin of the topological states, we refer to Ref. 29. Note that even when $U = 0$, while only quadratic terms of annihilation and creation operators appear in the Hamiltonian,

$\Delta \neq 0$ introduces nonzero matrix elements between states whose number of fermions differs by two. The dimension of the Hilbert space grows exponentially as the number of lattice sites L is increased, strongly limiting the availability of the exact diagonalization approach.

Suppose that we have a lattice system having two Majorana end modes $\hat{\gamma}_1, \hat{\gamma}_2$ such that $\eta^{\pm} \equiv \hat{\gamma}_1 \pm i\hat{\gamma}_2$ is a fermionic operator satisfying $(\eta^+)^\dagger = (\hat{\gamma}_1 + i\hat{\gamma}_2)^\dagger = \hat{\gamma}_1 - i\hat{\gamma}_2 = \eta^-$. If the Majorana operators can be approximated by linear combinations of the single-particle annihilation and creation operators, $\hat{\gamma}_j = \sum_{\sigma,l}[a^{(j)}_{\sigma,l}\hat{c}_{\sigma,l} + (a^{(j)}_{\sigma,l})^*\hat{c}^\dagger_{\sigma,l}]$ $(j = 1,2)$, then we can think of two single-particle wave functions, $|\gamma_j\rangle \equiv \sum_{\sigma,l}(a^{(j)}_{\sigma,l})^*\hat{c}^\dagger_{\sigma,l}|\rangle$, in which $|\rangle$ is the empty state, as the "Majorana wave functions." For the ground-state many-body wave functions in the sectors of total number of fermions being even (e) and odd (o), $|\Psi_{\mathrm{e,o}}\rangle$ with energies $E_{\mathrm{e,o}}$, we can obtain the values of $a^{(j=1,2)}_{\sigma,l}$ as follows:[20]

$$a^{(1)}_{\sigma,l} = \langle\Psi_\mathrm{o}|\hat{c}^\dagger_{\sigma,l}|\Psi_\mathrm{e}\rangle + \langle\Psi_\mathrm{e}|\hat{c}^\dagger_{\sigma,l}|\Psi_\mathrm{o}\rangle, \tag{3}$$

$$a^{(2)}_{\sigma,l} = \langle\Psi_\mathrm{o}|\hat{c}^\dagger_{\sigma,l}|\Psi_\mathrm{e}\rangle - \langle\Psi_\mathrm{e}|\hat{c}^\dagger_{\sigma,l}|\Psi_\mathrm{o}\rangle. \tag{4}$$

In Ref. 20, the phase diagrams for $U > 0$ and $U = 0$ are obtained by calculating $|\Psi_{\mathrm{e,o}}\rangle$ and checking if the following three conditions are met: (i) $\Delta E \equiv E_\mathrm{e} - E_\mathrm{o}$ vanishes; (ii) The left reduced density matrices of the system, obtained from the density matrices $|\Psi_{\mathrm{e(o)}}\rangle\langle\Psi_{\mathrm{e(o)}}|$ by tracing out all sites in the right half, have degenerate eigenvalue spectrum; and (iii) $\{a^{(1)}_{\sigma,l}\}$ and $\{a^{(2)}_{\sigma,l}\}$ are spatially localized to the different ends. Now we apply these conditions to the case with spatial inhomogeneity.

Quasiperiodic site potential. We study the effect of a quasiperiodic site potential, which is given by

$$\epsilon_{\sigma,l} = V_\mathrm{Q}\cos[\kappa(l - l_\mathrm{c}) + \delta], \tag{5}$$

in which $V_\mathrm{Q} \geqslant 0, l_\mathrm{c} \equiv (L-1)/2$, and the phase is $\delta = 0$ unless noted. We choose $\kappa = 2\pi g$, in which $g = \sqrt{5} - 2$.

In the noninteracting case ($U = \Delta = 0$), we can consider a periodic lattice with $g_n = F_{n-3}/F_n$, in which F_n is the nth Fibonacci number, to obtain the approximate eigenenergy distribution. The Fourier transform of the site potential then has only components with $k = \pm 2\pi g_n, \pm 2\pi(1 - g_n)$ but mixes states between the upper and lower RZ bands because the spin composition of the states in the RZ bands depends on the wave number. g_n rapidly converges to g as n is increased, as does the eigenvalue distribution. As V_Q is increased, the number and widths of the gaps in the eigenvalue distribution both increase. For $V_\mathrm{Q} \sim t$, the spectrum exhibits a distinct self-similar structure when κ is changed, which resembles two Hofstadter butterflies[30,31] shifted in energy and overlapping each other, as shown in the inset of Fig. 1(a). We note that for $\alpha = V_z = 0$, all single-body wave functions are extended for $V_\mathrm{Q} < t$ and localized for $V_\mathrm{Q} > t$ in the limit of large system $(L \to \infty)$.[30]

In Fig. 1, we plot ΔE against μ for several values of V_Q for $L = 200$ sites, as well as the eigenenergies of the noninteracting case with the quasiperiodic potential. The slope of the ΔE as a function of μ is often close to ± 1 outside the TS phase, which corresponds to the fact that $N_\mathrm{e} - N_\mathrm{o}$ is close to ∓ 1 in such regions of μ. The two regions with $\Delta E = 0$ for $V_\mathrm{Q} = 0$ correspond to the ranges of μ crossing only one

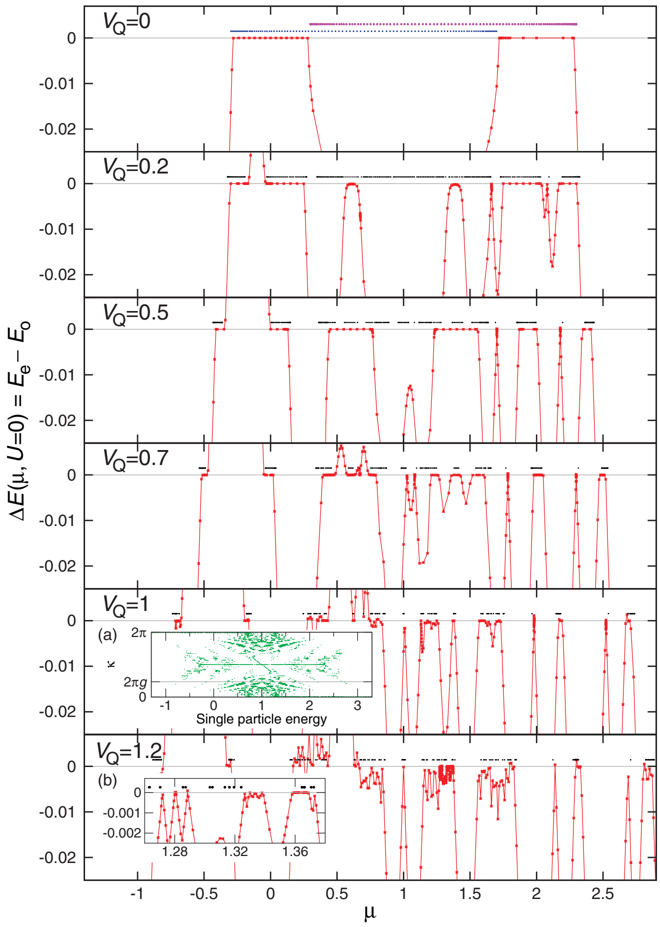

FIG. 1. (Color online) Differences in energy between the ground states in even and odd number sectors of the Hamiltonian plotted against the chemical potential μ. The energy spectrum of upper and lower RZ band eigenstates for the $L = 233$ case has been plotted in two lines above the horizontal $\Delta E = 0$ line for $V_\mathrm{Q} = 0$, and the single-particle energy spectrum of the $\Delta = 0$ case for $L = 200$ has been plotted above the $\Delta E = 0$ line for each value of $V_\mathrm{Q} = 0, 0.2, 0.5, 0.7, 1$, and 1.2. The other parameters are $(\Delta, \alpha, V_z) = (0.1, 0.3, 0.3)$ and $U = 0$. Insets: (a) The single-particle energy spectrum of the $\Delta = 0$ case plotted for $\kappa \in [0, 2\pi]$ and $V_\mathrm{Q} = 1$, and (b) a closeup of the main plot for $\mu \in [1.26 : 1.38]$ for $V_\mathrm{Q} = 1.2$.

of the two RZ bands. The RZ bands are gradually mixed and split into several minibands as V_Q is increased also for the open boundary condition. While the locations and widths of some of the regions with vanishing ΔE resemble those of the minibands, not all of the regions of the chemical potential overlapping with one of the minibands have $\Delta E = 0$. While the value of ΔE outside of the plateaus at ΔE depends on the choice of δ, the locations and widths of the plateaus almost do not change when δ is changed.

We have observed that the other two conditions of Ref. 20, namely, (ii) the localized end states and (iii) the degeneracy of reduced density-matrix eigenvalues, are satisfied in the regions in which ΔE vanishes, and they are not satisfied when $|\Delta E| \gtrsim 10^{-4}$. The amplitude distribution of the wave function of the end Majorana modes for $(V_\mathrm{Q}, \mu) = (0.2, 0.5)$ is shown in Fig. 2(a). The distributions of $|a^{(1)}|^2$ and $|a^{(2)}|^2$ are, respectively, localized to the right and left ends of the

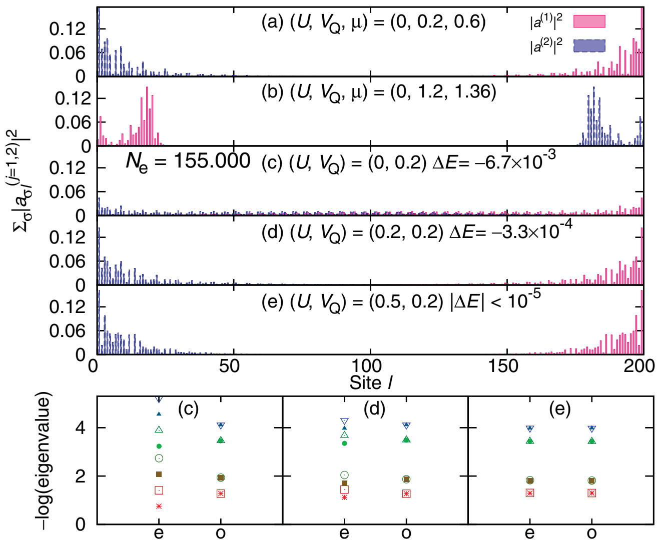

FIG. 2. (Color online) Top: The values of $\sum_\sigma |a_{\sigma,l}|^2$ are plotted against the site l for (a) $(U,V_Q,\mu) = (0,0.2,0.6)$, (b) $(U,V_Q,\mu) = (0,1.2,1.36)$, (c) $(U,V_Q,\mu) = (0,0.2,0.67448)$, (d) $(U,V_Q,\mu) = (0.2,0.2,0.75743)$, and (e) $(U,V_Q,\mu) = (0.5,0.2,0.85472)$. In (c)–(e), the value of μ has been chosen so that $N_e = 155.000$. Bottom: The eigenvalue spectra of the reduced density matrix for the left half of the system in states Ψ_e and Ψ_o are plotted for the parameter sets used in (c)–(e).

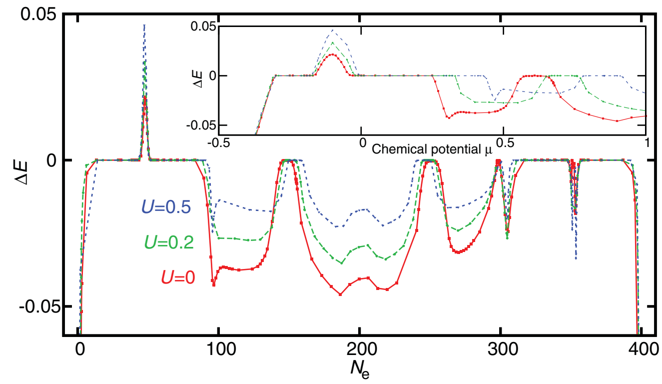

FIG. 3. (Color online) The energy difference between ground states in the sectors with even and odd number of fermions plotted against the number of fermions for $U = 0,0.2$, and 0.5. The other parameters are $(\Delta,\alpha,V_z) = (0.1,0.3,0.3)$ and $V_Q = 0.2$. Inset: the same plotted against the chemical potential μ.

system. While for $V_Q \gtrsim 1$, the plots of $\Delta E(\mu,U = 0)$ exhibit significantly shorter plateaus at $\Delta E = 0$, the two Majorana modes localized at the two ends are observed inside such plateaus, as shown for $(V_Q,\mu) = (1.2,1.36)$ in Fig. 2(b). This is a nontrivial observation because for $|V_Q| > 1$ we expect localized single-particle states for $\Delta = 0$, and localized states would not support global TSs. The reduced density-matrix eigenvalues are also degenerate, therefore we conclude that a TS with end Majorana fermions is realized in the $\Delta E = 0$ plateaus. We have also observed that the dependence of the regions with Majorana end states on the initial phase δ is weak in our system, which is similar to the noninteracting case,[15] while the sign of ΔE between these regions depends on the choice of δ.

While we easily obtain the Bogoliubov quasiparticle energies by retaining the value of Δ and diagonalizing the Hamiltonian in the Nambu spinor space,[11] the correspondence between the degenerate region and the single band region in the quasiparticle spectrum has been observed to be comparable at best to the correspondence between the former and the single band region of the minibands without Δ. We believe that not only the energy spectrum but also the spatial distribution of the states is important in the realization of the TS states.

In the studies of 1D topological phases of *free* fermions in bichromatic superlattices,[15,16] the topological phases appear only at special filling factors between the bulk bands. Here we emphasize that in our system of the 1D quantum wire with strong SOI, placed under a magnetic field and having a proximity-induced pairing, the topological phases are realized in several finite ranges of μ that correspond to finite ranges of the filling factor, as observed in Figs. 1 and 3 ($U = 0$), with some of them much closer to half filling compared to the $V_Q = 0$ case. This is the main result of this Rapid Communication.

Effect of fermion-fermion interaction. Next we study the effect of an on-site fermion-fermion interaction coexisting with the quasiperiodic site potential modulation. In Fig. 3, the values of $\Delta E(\mu,U)$ for $U = 0,0.2$, and 0.5 are plotted against the number of fermions N_e in the system, as well as against μ.

When U is larger, the amount of increase in μ required for adding the same number of fermions at the same filling factor becomes larger because of the stronger repulsive interaction. The $\Delta E(\mu) = 0$ plateaus in the inset of Fig. 3 are observed in broader ranges of the chemical potential, as expected from Ref. 20, with $V_Q = 0$. Furthermore, we observe that the plateaus are broader for larger U also in terms of the number of fermions.[32]

For a fixed N_e, chosen so that ΔE approaches zero as U is increased, in Figs. 2(c)–2(e) we observe that the distributions of $|a^{(j)}_{\sigma,l}|$ become localized toward the ends. We also observe that the difference between the eigenstate spectra of the reduced density matrices for Ψ_e and Ψ_o, plotted in the bottom part of Fig. 2, becomes smaller as ΔE becomes smaller. Similar behavior of the distributions of $|a^{(j)}_{\sigma,l}|$ and the eigenstate spectra of the reduced density matrices are observed in other plateaus of $\Delta E(\mu,U)$.

Effect of a trapping potential. In many cold-atom experiments, atom clouds are trapped in the vacuum by (magneto)optical potentials that are better approximated by a harmonic or Gaussian potential rather than a flat, boxlike potential. Also, in condensed-matter systems, the shape of the potential for electrons in the quantum wire would depend on how it is fabricated. Studying the effect of an additional trapping potential on the realization of the Majorana end fermions is therefore important and has already been conducted for noninteracting cases.[15,16] To complete this Rapid Communication, we study the effect of a harmonic potential, $V_H[(l - l_c)/l_c]^2$ $(l = 0,1,\ldots,L - 1 = 2l_c)$, added to the site potential (5).

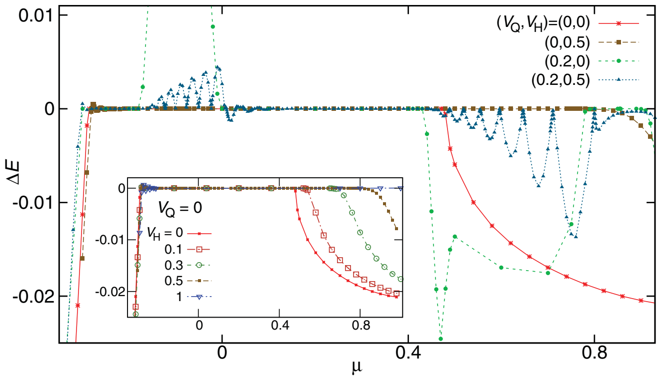

FIG. 4. (Color online) ΔE plotted against μ for $(V_Q,V_H) = (0,0),(0,0.5),(0.2,0)$, and $(0.2,0.5)$. The other parameters are $(\Delta,\alpha,V_z,U) = (0.1,0.3,0.3,0.5)$. Inset: ΔE plotted against μ for $V_Q = 0$ and $V_H = 0,0.1,0.3,0.5$, and 1.

Figure 4 shows ΔE plotted against μ for $(V_Q,V_H) = (0,0),(0,0.5),(0.2,0)$, and $(0.2,0.5)$ with $(\Delta,\alpha,V_z,U) = (0.1,0.3,0.3,0.5)$. The first three plateaus at $\Delta E = 0$ for $(V_Q,V_H) = (0.2,0)$ are in the plot. We observe that between these plateaus, ΔE plotted for $(V_Q,V_H) = (0.2,0.5)$ shows repeated oscillations.

In the inset of Fig. 4 we have plotted ΔE for $V_Q = 0$ and several values of V_H. For increasing V_H, the first region of vanishing ΔE is broadened. The Majorana fermion states are localized close to the system boundary, where the harmonic trap decreases the effective chemical potential, measured from the local site potential, by almost the depth of the trap potential V_H. This explains the increase of the value of μ at the upper boundary.

On the other hand, our system with the quasiperiodic potential has the Majorana state broken down not only between the plateau for the system with $(V_Q,V_H) = (0.2,0)$, but also inside the second and third plateaus, when V_H is introduced. We believe that this is because the values of the effective chemical potential at which the quasiperiodic potential destroys the TS is reached at some location even for greater values of μ for $V_H > 0$. This effect seems to compete with the decrease of the effective chemical potential at the edge of the fermion distribution and ΔE oscillates. While for simplicity we have shown here the results for the case with $U = 0.5$, the discussion above is also consistent with those for other values of $U \geqslant 0$.

In conclusion, we have studied the effect of spatial inhomogeneity realized by a quasiperiodic site potential modulation applied on a tight-binding model of a TS, which is a 1D conductor with SOI in the proximity of a bulk superconductor and under a magnetic field. When the modulation is induced, the topological phase appears not only when the band is almost empty or almost full, but also in several regions of the filling factor (or the chemical potential) with finite widths much closer to half filling, even when the modulation is strong enough to turn the system without SOI and pairing insulating. We have also studied the effects of on-site fermion-fermion interaction and a harmonic trap. Without the trap, as the interaction becomes stronger, the TS phase becomes wider in the phase diagram, as in the case without the spatial inhomogeneity,[20] in terms of both the chemical potential and the number of fermions in the system. Our results reveal the possibility of realizing Majorana end states in 1D systems such as cold-atom systems and superconductor-metal heterostructures with inherent or imposed inhomogeneities.

Recently, we became aware that the interplay of disorder and correlation in 1D TSs has also been investigated in Ref. 33.

This work was partially supported by the Grant-in-Aid for the Global COE Program "The Next Generation of Physics, Spun from Universality and Emergence" from MEXT of Japan. N.K. is supported by KAKENHI (Grants No. 21540359 and No. 20102008) and JSPS through its FIRST Program. Part of the computation in this work has been performed using the facilities of the Supercomputer Center, Institute for Solid State Physics, University of Tokyo.

*tezuka@scphys.kyoto-u.ac.jp

[1] N. Read and D. Green, Phys. Rev. B **61**, 10267 (2000).
[2] A. Yu. Kitaev, Phys. Usp. **44**, 131 (2001).
[3] D. A. Ivanov, Phys. Rev. Lett. **86**, 268 (2001).
[4] L. Fu and C. L. Kane, Phys. Rev. Lett. **100**, 096407 (2008).
[5] M. Sato, Y. Takahashi, and S. Fujimoto, Phys. Rev. Lett. **103**, 020401 (2009).
[6] Y. Tanaka, T. Yokoyama, and N. Nagaosa, Phys. Rev. Lett. **103**, 107002 (2009); J. Linder, Y. Tanaka, T. Yokoyama, A. Sudbø, and N. Nagaosa, *ibid.* **104**, 067001 (2010); Y. Tanaka, M. Sato, and N. Nagaosa, J. Phys. Soc. Jpn. **81**, 011013 (2012); A. Yamakage, Y. Tanaka, and N. Nagaosa, Phys. Rev. Lett. **108**, 087003 (2012).
[7] S. Tewari, S. Das Sarma, C. Nayak, C. Zhang, and P. Zoller, Phys. Rev. Lett. **98**, 010506 (2007).
[8] J. D. Sau, R. M. Lutchyn, S. Tewari, and S. Das Sarma, Phys. Rev. Lett. **104**, 040502 (2010).
[9] J. Alicea, Phys. Rev. B **81**, 125318 (2010).
[10] R. M. Lutchyn, J. D. Sau, and S. Das Sarma, Phys. Rev. Lett. **105**, 077001 (2010).
[11] Y. Oreg, G. Refael, and F. von Oppen, Phys. Rev. Lett. **105**, 177002 (2010).
[12] O. Motrunich, K. Damle, and D. A. Huse, Phys. Rev. B **63**, 224204 (2001).
[13] I. A. Gruzberg, N. Read, and S. Vishveshwara, Phys. Rev. B **71**, 245124 (2005).
[14] P. W. Brouwer, M. Duckheim, A. Romito, and F. von Oppen, Phys. Rev. Lett. **107**, 196804 (2011).
[15] L.-J. Lang, X. Cai, and S. Chen, e-print arXiv:1110.6120.
[16] F. Mei, S.-L. Zhu, Z.-M. Zhang, C. H. Oh, and N. Goldman, Phys. Rev. A **85**, 013638 (2012).
[17] B. Braunecker, G. I. Japaridze, J. Klinovaja, and D. Loss, Phys. Rev. B **82**, 045127 (2010).
[18] L. Fidkowski and A. Kitaev, Phys. Rev. B **81**, 134509 (2010).

[19] S. Gangadharaiah, B. Braunecker, P. Simon, and D. Loss, Phys. Rev. Lett. **107**, 036801 (2011).

[20] E. M. Stoudenmire, J. Alicea, O. A. Starykh, and M. P. A. Fisher, Phys. Rev. B **84**, 014503 (2011).

[21] E. Sela, A. Altland, and A. Rosch, Phys. Rev. B **84**, 085114 (2011).

[22] R. M. Lutchyn and M. P. A. Fisher, Phys. Rev. B **84**, 214528 (2011).

[23] G. Roati *et al.*, Nature (London) **453**, 895 (2008).

[24] E. Lucioni, B. Deissler, L. Tanzi, G. Roati, M. Zaccanti, M. Modugno, M. Larcher, F. Dalfovo, M. Inguscio, and G. Modugno, Phys. Rev. Lett. **106**, 230403 (2011).

[25] A. C. Potter and P. A. Lee, Phys. Rev. Lett. **105**, 227003 (2010); Phys. Rev. B **83**, 094525 (2011).

[26] R. M. Lutchyn, T. D. Stanescu, and S. Das Sarma, Phys. Rev. Lett. **106**, 127001 (2011); T. D. Stanescu, R. M. Lutchyn, and S. Das Sarma, Phys. Rev. B **84**, 144522 (2011).

[27] S. R. White, Phys. Rev. Lett. **69**, 2863 (1992); Phys. Rev. B **48**, 10345 (1993).

[28] U. Schollwöck, Ann. Phys. **326**, 96 (2011).

[29] M. Sato, Y. Takahashi, and S. Fujimoto, Phys. Rev. B **82**, 134521 (2010).

[30] M. Kohmoto, Phys. Rev. Lett. **51**, 1198 (1983); C. Tang and M. Kohmoto, Phys. Rev. B **34**, 2041 (1986).

[31] D. R. Hofstadter, Phys. Rev. B **14**, 2239 (1976).

[32] N_{e} and N_{o} are both increasing functions of μ. While they are degenerate only inside the topological insulator phase, $|N_{\mathrm{e}} - N_{\mathrm{o}}|$ is observed to be at most unity. Therefore the widths of the $\Delta E = 0$ plateaus are not significantly changed if we choose to plot ΔE against N_{o}.

[33] A. M. Lobos, R. M. Lutchyn, and S. Das Sarma, e-print arXiv:1202.2837.